# Optimal Design of Nonlinear Series Elastic Actuator for Minimization of Actuator Power

Nicolas Schmit and Masafumi Okada*†

In this paper, we propose a methodology to optimize the nonlinear stiffness of nonlinear Series Elastic Actuators (SEAs). The nonlinear restoring forces of the springs are optimized in order to minimize the mechanical power of the actuators of the SEAs. We define the cost function as the time average of the square of the actuator power, and use a 3rd order Hermite interpolation to parameterize the restoring force of the nonlinear springs. The cost function is optimized using a Sequential Quadratic Programming (SQP) algorithm. We detail the bounds on the design parameters and the nonlinear optimization constraints. We show an example of optimal design in the case of a 3 Degree Of Freedom (DOF) manipulator, and in the last section we show that the optimal nonlinear springs calculated for this manipulator can be realized using a non-circular cable-spool mechanism.

**Keywords:** *series elastic actuator, nonlinear spring, optimal design, robotic manipulator*

## 1. INTRODUCTION

SEAs are made by coupling an actuator, like a motor connected to a gear train, in series with an elastic element [1], as shown in Fig. 1. SEAs can be used as force actuators, by controlling the displacement of the spring and knowing its stiffness [2], or be used as programmable springs, by imposing a particular relationship between the displacement of the actuator and the displacement of the spring [3].

One of the advantages of SEAs are that they have low impedance, the motor is isolated from shock loads, and the effects of backlash, torque ripple, and friction are filtered by the spring [1]. As SEAs are force controllable actuators, they are safer to use with human subjects as opposed to direct drive systems that are position controlled [4, 5]. Another advantage of SEAs are the ability to store energy in the spring as potential energy, thus reducing the total energy consumption in the case of cyclic motions such as running [6, 7] and dribbling [8].

A sub-category of SEAs are those that use nonlinear springs. In shock absorption mechanisms, a hardening spring results in appreciably lower displacements and significantly higher accelerations than a linear spring, whereas a softening spring might be advisable when the structural element to be protected is unable to withstand high accelerations and the restrictions on the maximum deflections are not very stringent [9]. Nonlinear springs can be used to create a force limiter, so that the stiffness of the joint drops if the force exceeds a given threshold [10]. SEAs with quadratic stiffness are used in antagonistic configuration to create Variable Stiffness Actuators (VSAs) where the force and the stiffness can be tuned independently [5, 11, 12].

So far, very few have been said about how to optimize the springs of nonlinear SEAs. In [13], the authors developed a nonlinear SEA where the nonlinear stiffening spring is optimized for the nonlinearities typically found in revolute-jointed hopping robots. In [14], the authors proposed a method to optimize the stiffness of a mechanism in order to to minimize the energy consumption, but this method is limited to linear stiffness. In [15], the authors proposed a methodology to optimize the design of nonlinear springs that work in parallel with the actuators, but this methodology cannot be used when the springs are in series with the actuators.

In this paper, we propose a general methodology to optimize the nonlinear springs of nonlinear SEAs in order to minimize the mechanical power of the actuators. First, we define the cost function as the time average of the square of the actuator mechanical power, then we use an 3rd order Hermite interpolation (piecewise 3rd order polynomial interpolation) to express the restoring force of the nonlinear springs, and finally we use a SQP algorithm to find the data points of the interpolation that minimize the cost function. On a simple example of optimal design of a 3 DOF

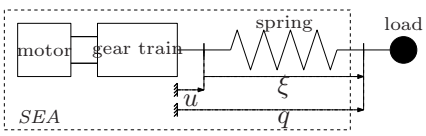


**Fig.**1 Series Elastic Actuator.

*This research is supported by the *Research on Macro/Micro Modeling of Human Behavior in the Swarm and its Control* under the Core Research for Evolutional Science and Technology (CREST) Program (research area: Advanced Integrated Sensing Technologies), Japan Science and Technology Agency (JST).

†The authors are with the Department of Mechanical Sciences and Engineering, Tokyo Institute of Technology, 2-12-1 Ookayama, Meguro-ku, 152-8550 Tokyo, Japan schmit.n.aa@m.titech.ac.jp

serial manipulator, we show that the use of nonlinear springs in the SEAs leads to a smaller energy consumption compared to when using linear springs. Finally, in the last section, we show that the optimal nonlinear springs calculated for this manipulator can be realized using a non-circular cable-spool mechanism.

## 2. Problem statement

We consider a robot with $n$ DOFs. Each joint is actuated by a nonlinear SEA as shown in Fig. 1. The output of the motor is connected to the input of the gear train, the output of the gear train is connected to one side of a nonlinear spring, and the other side of the nonlinear spring is connected to the load. $u$ is the position of the output of the gear train, $q$ is the position of the mechanical joint and $\xi$ is the displacement of the spring.

Assuming that the mass-inertia parameters of the nonlinear springs are negligible compared with those of the system elements, the equations of motion of the robot can be written as

$$\forall i \in \{1..n\}, \frac{d}{dt}\left(\frac{\partial K}{\partial \dot{q}_i}\right) - \frac{\partial K}{\partial q_i} + \frac{\partial P}{\partial q_i} = -w_i(\xi_i) - c_i\dot{q}_i \tag{1}$$

Where the subscript $i$ means the $i^{\text{th}}$ joint, $K$ is the kinetic energy, $P$ is the potential energy, $w_i(\xi_i)$ is the restoring force[1] of the nonlinear spring of the $i^{\text{th}}$ joint, $c_i$ is the viscous friction of the joint and $\dot{q}_i$ stands for the time-derivative of $q_i$. We assume that the joint trajectory $q(t)$, speed $\dot{q}(t)$, acceleration $\ddot{q}(t)$, time-derivative of acceleration $\dddot{q}(t)$, the viscous friction $c_i$ and the expression of the kinetic energy $K$ and potential energy $P$ are known. We define the function $\mathcal{G}_i(t)$ as

$$\mathcal{G}_i(t) = \frac{d}{dt}\left(\frac{\partial K}{\partial \dot{q}_i}\right) - \frac{\partial K}{\partial q_i} + \frac{\partial P}{\partial q_i} + c_i\dot{q}_i \tag{2}$$

As a consequence to (1)

$$w_i(\xi_i(t)) = -\mathcal{G}_i(t) \tag{3}$$

The function $\mathcal{G}_i(t)$ is known, but the functions $\xi_i(t)$ (displacement of the spring vs. time) and $w_i(\xi_i)$ (restoring force of the spring) are unknown.

We want to optimize the nonlinear springs to minimize the mechanical power of the actuators. We define the cost function of the optimization problem as the sum of the time average of the square of the actuators' mechanical power.

$$\mathcal{C} = \sum_{i=1}^{n}\left[\frac{1}{T}\int_0^T \underbrace{\left(w_i(\xi(t))\dot{u}_i(t)\right)}_{\text{actuator power}}^2 dt\right] \tag{4}$$

[1] We use the word "force" to design either a force in the case of a prismatic joint or a torque in the case of a revolute joint. Indeed, the equations are the same for prismatic and revolute joints.

Using the notations of Fig. 1, $\dot{u}_i(t)$ is obtained as

$$\dot{u}_i(t) = \dot{q}_i(t) - \dot{\xi}_i(t) \tag{5}$$

By taking the time derivative of (3), we obtain

$$w_i'(\xi_i(t))\,\dot{\xi}_i(t) = -\dot{\mathcal{G}}_i(t) \tag{6}$$

where $w_i'(\xi_i)$ stands for $\frac{dw_i(\xi_i)}{d\xi_i}$. We assume that the stiffness of the nonlinear springs is strictly positive[2] ($w_i'(\xi_i) > 0$). Substituting (3), (5), (6), in (4), we obtain

$$\mathcal{C} = \sum_{i=1}^{n}\left[\frac{1}{T}\int_0^T \mathcal{G}_i^2(t)\left(\dot{q}_i(t) + \frac{\dot{\mathcal{G}}_i(t)}{w_i'(\xi_i(t))}\right)^2 dt\right] \tag{7}$$

## 3. Parameterization of the optimization problem

### 3.1 Expression of the cost function with the normalized restoring force

We consider the normalized spring displacement $\overline{\xi}_i$ and normalized restoring force $\overline{w}_i(\overline{\xi}_i)$. $\overline{\xi}_i$ and $\overline{w}_i(\overline{\xi}_i)$ are mapped to $\xi_i$ and $w_i(\xi_i)$ respectively by the relationships

$$\xi_i = \Xi_i\overline{\xi}_i \tag{8}$$

$$w_i(\xi_i) = w_{i,\min} + (w_{i,\max} - w_{i,\min})\,\overline{w}_i\left(\overline{\xi}_i\right) \tag{9}$$

where

$$w_{i,\min} = \min_{t\in[0,T]}(-\mathcal{G}_i(t)) \tag{10}$$

$$w_{i,\max} = \max_{t\in[0,T]}(-\mathcal{G}_i(t)) \tag{11}$$

and $\Xi_i$ is the displacement range of the $i^{\text{th}}$ nonlinear spring. Both $\overline{\xi}_i$ and $\overline{w}_i(\overline{\xi}_i)$ are dimensionless and take their values between 0 and 1. Since we assumed in Section 2. that the stiffness of each nonlinear spring is strictly positive, $\overline{w}_i(\overline{\xi}_i)$ is a monotonically increasing function. Furthermore, (9) imposes

$$\overline{w}_i(0) = 0 \tag{12}$$

$$\overline{w}_i(1) = 1 \tag{13}$$

By taking the derivative of (9) with respect to $\xi_i$, we obtain

$$w_i'(\xi_i) = \frac{w_{i,\max} - w_{i,\min}}{\Xi_i}\,\overline{w}_i'\left(\overline{\xi_i}\right) \tag{14}$$

where $\overline{w}_i'(\overline{\xi}_i)$ stands for $\frac{d\overline{w}_i(\overline{\xi}_i)}{d\overline{\xi}_i}$. Since $\overline{w}_i(\overline{\xi}_i)$ is a monotonically increasing function, it is invertible:

$$\overline{\xi}_i(t) = \overline{w}_i^{-1}(\overline{w}_i) \tag{15}$$

[2] During the optimization, we impose a constraint on the design parameters of the springs so that the stiffness is strictly positive. See Section 4.1 for the calculation of this constraint.

Where $\overline{w}_i^{-1}(\bullet)$ stands for the inverse function of $\overline{w}_i(\bullet)$. From (9), $\overline{w}_i$ is calculated as

$$\overline{w}_i = \frac{w_i - w_{i,\min}}{w_{i,\max} - w_{i,\min}} \tag{16}$$

We successively substitute (14), (15), (16) and (3) in (7), and obtain

$$\mathcal{C} = \sum_{i=1}^{n} \left[ \frac{1}{T} \int_0^T \mathcal{G}_i^2(t) \left( \dot{q}_i(t) + \Xi_i \mathcal{H}_i(t) \right)^2 dt \right] \tag{17}$$

with

$$\mathcal{H}_i(t) = \frac{\dot{\mathcal{G}}_i(t)}{(w_{i,\max} - w_{i,\min})\, \overline{w}_i' \left( \overline{w}_i^{-1} \left( \frac{\mathcal{G}_i(t) + w_{i,\min}}{w_{i,\min} - w_{i,\max}} \right) \right)} \tag{18}$$

### 3.2 Parameterization of the normalized spring force function

$\overline{w}_i(\overline{\xi}_i)$ is parameterized using the method presented in [16]. As mentioned previously, $\overline{\xi}_i$ takes its values in $[0, 1]$. This interval is divided into $N$ equal subintervals of length $1/N$ ($\overline{\xi}_i$ is dimensionless). These intervals define $N + 1$ nodes:

$$z_j = \frac{j-1}{N}, \quad j \in \{1..N+1\} \tag{19}$$

A 3rd order polynomial is used to represent the force $\overline{w}_i(\overline{\xi}_i)$ on each subinterval. The value of $\overline{w}_i$ and its derivative $\overline{w}_i'$ at the nodes $z_j$ are used as design parameters. For each subinterval, the unique 3rd order polynomial is defined that has values $(f_{i,j}, f_{i,j+1})$ and derivatives $(s_{i,j}, s_{i,j+1})$ at the end points of $[z_j, z_{j+1})$. This definition allows the normalized restoring force any point $z = z_j + \frac{\rho_i}{N}$ in $[z_j, z_{j+1})$ to be written as

$$\underset{\overline{\xi}_i \in [z_j, z_{j+1})}{\overline{w}_i(\overline{\xi}_i)} = \alpha_i\, f_{i,j+1} + \beta_i\, f_{i,j} + \frac{\gamma_i\, s_{i,j+1} + \delta_i\, s_{i,j}}{N} \tag{20}$$

where $\alpha_i$, $\beta_i$, $\gamma_i$, $\delta_i$ are calculated as

$$\alpha_i = \rho_i^2(3 - 2\rho_i) \quad (21) \qquad \gamma_i = \rho_i^2(\rho_i - 1) \quad (23)$$
$$\beta_i = 2\rho_i^3 - 3\rho_i^2 + 1 \quad (22) \qquad \delta_i = \rho_i(\rho_i - 1)^2 \quad (24)$$

$$\rho_i = N\,\overline{\xi}_i \mod 1 \tag{25}$$

This scheme, called Hermite interpolation, automatically gives continuity of $\overline{w}_i(\overline{\xi}_i)$ and its derivative at the nodes. An example of the interpolation of $\overline{w}_i(\overline{\xi}_i)$ is shown in Fig. 2.

### 3.3 Calculation of $\overline{w}_i'(\overline{\xi}_i)$ and $\overline{w}_i^{-1}(\overline{w}_i)$

In order to calculate $\mathcal{H}(t)$, we need the expression of the functions $\overline{w}_i'(\overline{\xi}_i)$ and $\overline{w}_i^{-1}(\overline{w}_i)$. By taking the derivative of (20) with respect to $\overline{\xi}_i$, $\overline{w}_i'(\overline{\xi}_i)$ is calculated as

$$\underset{\overline{\xi}_i \in [z_j, z_{j+1})}{\overline{w}_i'(\overline{\xi}_i)} = N\left(\alpha_i'\, f_{i,j+1} + \beta_i'\, f_{i,j}\right) + \gamma_i'\, s_{i,j+1} + \delta_i'\, s_{i,j} \tag{26}$$

with

$$\alpha_i' = 6\rho_i(1 - \rho_i) \quad (27) \qquad \gamma_i' = 3\rho_i^2 - 2\rho_i \quad (29)$$
$$\beta_i' = 6\rho_i(\rho_i - 1) \quad (28) \qquad \delta_i' = 3\rho_i^2 - 4\rho_i + 1 \quad (30)$$

$\rho_i$ is calculated using (25).

To calculate $\overline{\xi}_i = \overline{w}_i^{-1}(\overline{w}_i)$, we first determine the integer $j$ such as

$$f_{i,j} \leqslant \overline{w}_i < f_{i,j+1} \tag{31}$$

we substitute (21), (22), (23) and (24) in (20) and rewrite (20) as

$$a\rho_i^3 + b\rho_i^2 + c\rho_i + d = 0 \tag{32}$$

with the coefficients of the polynomial

$$a = -2f_{i,j+1} + 2f_{i,j} + \frac{s_{i,j+1}}{N} + \frac{s_{i,j}}{N} \tag{33}$$
$$b = 3f_{i,j+1} - 3f_{i,j} - \frac{s_{i,j+1}}{N} - 2\frac{s_{i,j}}{N} \tag{34}$$
$$c = \frac{s_{i,j}}{N} \tag{35}$$
$$d = f_{i,j} - \overline{w}_i \tag{36}$$

Since $\overline{w}_i(\overline{\xi}_i)$ is a monotonically increasing function, the polynomial (32) has a unique real root in $[0, 1]$. From the root $\rho_i$ of (32), $\overline{\xi}_i$ is calculated as

$$\overline{\xi}_i = \frac{j - 1 + \rho_i}{N} \tag{37}$$

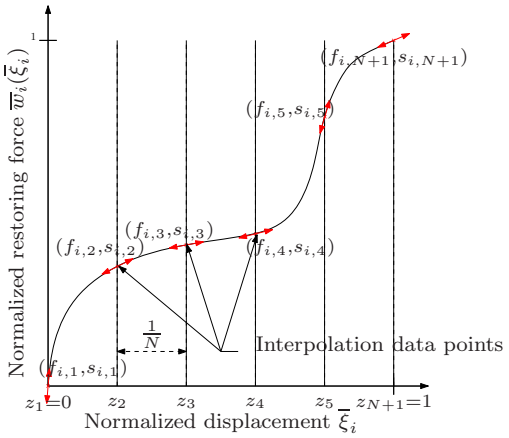


**Fig.**2 Parameterization of the normalized restoring force $\overline{w}_i(\overline{\xi}_i)$ using a Hermite interpolation. The value of $\overline{w}_i$ and its derivative $\overline{w}_i'$ at the nodes $z_j$ are used as design parameters. On each subinterval, $\overline{w}_i(\overline{\xi}_i)$ is expressed by a third order polynomial uniquely defined by its values and derivatives at the endpoints of the subinterval.

So far, we defined for each nonlinear spring three kinds of design parameters:

- The value of $\overline{w}_i(\overline{\xi}_i)$ at the interpolation nodes: $f_{i,j}$
- The value of $\overline{w}'_i(\overline{\xi}_i)$ at the interpolation nodes: $s_{i,j}$
- The displacement range of the nonlinear spring: $\Xi_i$

However, the definition of $\overline{w}_i(\overline{\xi}_i)$ imposes $f_{i,1} = 0$ and $f_{i,N+1} = 1$. Consequently, the vector of design parameters for the $i^{\text{th}}$ nonlinear spring is

$$y_i = [f_{i,2}, ..., f_{i,N}, s_{i,1}, ..., s_{i,N+1}, \Xi_i] \tag{38}$$

In (17) each integral term depends only on the design parameters of one single spring. Therefore, we can solve the optimization problem for each DOF one by one.

$$\forall i \in \{1..n\}, \min_{y_i \in \Omega_i} \left\{ \frac{1}{T} \int_0^T \mathcal{G}_i^2(t) \left(\dot{q}_i(t) + \Xi_i \mathcal{H}_i(t)\right)^2 dt \right\} \tag{39}$$

where $\Omega_i$ is the set of $y_i$ satisfying all the design constraints and bounds (defined in next section).

## 4. Constraints, bounds and initialization of the design parameters

### 4.1 Nonlinear constraints to bound the stiffness of the nonlinear springs

In order to control the stiffness of the nonlinear springs, we add the following nonlinear constraints

$$\forall i \in \{1..n\}, \forall \overline{\xi}_i \in [0,1], \overline{w}'_i(\overline{\xi}_i) \geqslant \overline{w}'_{\min} \tag{40}$$

$$\forall i \in \{1..n\}, \forall \overline{\xi}_i \in [0,1], \overline{w}'_i(\overline{\xi}_i) \leqslant \overline{w}'_{\max} \tag{41}$$

The parameters $\overline{w}'_{\min}$ and $\overline{w}'_{\max}$ can be chosen by the designer within the following range

$$0 < \overline{w}'_{\min} \leqslant 1 \tag{42}$$

$$1 \leqslant \overline{w}'_{\max} < \infty \tag{43}$$

The closer $\overline{w}'_{\min}$ and $\overline{w}'_{\max}$ to 1, the more linear the springs. The constraint $0 < \overline{w}'_{\min}$ is critical to ensure that the inverse function (15) is always defined. Using (26) to calculate $\overline{w}'_i(\overline{\xi}_i)$, (40) is equivalent to

$$\forall i \in \{1..n\} \forall j \in \{1..N\}, \max_{\rho \in [0,1]} \left\{ a_{i,j}\rho^2 + b_{i,j}\rho + c_{i,j} \right\} \leqslant 0 \tag{44}$$

with

$$a_{i,j} = 6f_{i,j+1} - 6f_{i,j} - 3\frac{s_{i,j+1}}{N} - 3\frac{s_{i,j}}{N} \tag{45}$$

$$b_{i,j} = -6f_{i,j+1} + 6f_{i,j} + 2\frac{s_{i,j+1}}{N} + 4\frac{s_{i,j}}{N} \tag{46}$$

$$c_{i,j} = \frac{\overline{w}'_{\min}}{N} - \frac{s_{i,j}}{N} \tag{47}$$

To express the constraint (44), we calculate the maximum of the polynomial $a_{i,j}\rho^2 + b_{i,j}\rho + c_{i,j}$ on $[0,1]$. (44) is equivalent to

$$\forall i \in \{1..n\} \forall j \in \{1..N\}, \mathcal{P}_{i,j} \leqslant 0 \tag{48}$$

where the term $\mathcal{P}_{i,j}$ is calculated the following way:

- if $a_{i,j} > 0$, $\mathcal{P}_{i,j} = \max(c_{i,j}, a_{i,j} + b_{i,j} + c_{i,j})$
- if $a_{i,j} < 0$
  - if $-\frac{b_{i,j}}{2a_{i,j}} \leqslant 0$, $\mathcal{P}_{i,j} = c_{i,j}$
  - if $-\frac{b_{i,j}}{2a_{i,j}} \geqslant 1$, $\mathcal{P}_{i,j} = a_{i,j} + b_{i,j} + c_{i,j}$
  - if $0 < -\frac{b_{i,j}}{2a_{i,j}} < 1$, $\mathcal{P}_{i,j} = c_{i,j} - \frac{b_{i,j}^2}{4a_{i,j}}$
- if $a_{i,j} = 0$
  - if $b_{i,j} \geqslant 0$, $\mathcal{P}_{i,j} = b_{i,j} + c_{i,j}$
  - if $b_{i,j} < 0$, $\mathcal{P}_{i,j} = c_{i,j}$

The constraint (41) can be expressed in a similar way as (48) by replacing $\overline{w}'_{\min}$ with $\overline{w}'_{\max}$ in (47) and replacing $a_{i,j}$ with $-a_{i,j}$, $b_{i,j}$ with $-b_{i,j}$, and $c_{i,j}$ with $-c_{i,j}$ in the calculation of $\mathcal{P}_{i,j}$.

Since (40) and (41) constrain the normalized restoring force, these constraints are independent of the displacement range and load range of the spring. Consequently, no initial guess on the displacement and load range is required to choose the parameters $\overline{w}'_{\min}$ and $\overline{w}'_{\max}$.

### 4.2 Bounds

We impose the following bounds on the design parameters

$$0 \leqslant f_{i,j} \leqslant 1 \tag{49}$$

$$\overline{w}'_{\min} \leqslant s_{i,j} \leqslant \overline{w}'_{\max} \tag{50}$$

$$\Xi_{i,\min} \leqslant \Xi_i \leqslant \Xi_{i,\max} \tag{51}$$

(49) is imposed by the definition of $\overline{w}_i(\overline{\xi}_i)$. (50) is redundant with (40) and (41) but is required by the optimization algorithm to know in which interval to look for the $s_{i,j}$. The parameters $\Xi_{i,\min}$ and $\Xi_{i,\max}$ can be chosen by the designer within the following range, depending on design requirements.

$$0 < \Xi_{i,\min} < \Xi_{i,\max} < \infty \tag{52}$$

### 4.3 Optimization

We use the SQP [17] algorithm of Matlab to find the vectors of design parameters (38) which elements belong to the intervals defined in (49), (50), (51) which minimize the cost function (17) under the conditions (40) (41). Before starting the optimization algorithm, the design parameters (38) are initialized with the following values

- $f_{i,j} = \frac{j-1}{N}$
- $s_{i,j} = 1$
- $\Xi_i = \Xi_{i,\max}$

These parameters correspond to linear springs with the maximum displacement ranges allowed by (51).

## 5. Example of optimal design

We consider the 3-DOF serial manipulator shown in Fig. 3. $\ell_i$ is the length of link $i$, $h_i$ is the distance from the origin of the coordinate frame attached to link $i$ to the link's center of mass, $q_i$ is the angular displacement of coordinate frame $i$ with respect to coordinate frame $(i-1)$ (coordinate frame 0 is the reference frame), and $g$ is the acceleration of gravity.

We consider the joint trajectory shown in Fig. 4(a). The corresponding path of the end effector is shown in Fig. 4(b). We calculate the 3 nonlinear springs (one for each joint) which minimize the cost function (17). The user-defined parameters, such as the number of nodes to interpolate the spring restoring force function and the minimum/maximum stiffness are set as shown in Table 1.

In the left column of Fig. 5, we show the torque profile (torque vs. angular position) of the nonlinear springs of each joint. The vertical dash-dotted lines show the location of the interpolation nodes. In the right column of Fig. 5, we compare the displacement of the nonlinear spring (blue solid curve), the angular position of the joint (green dash-dotted curve), and the angular position of the actuator (red dashed curve) versus time. In order to evaluate how much energy is saved by using nonlinear springs in series with the actuators, we calculate the average absolute mechanical power of each actuator using the expression.

$$\langle |W_i| \rangle = \frac{1}{T} \int_0^T |w_i(\xi(t)) \dot{u}_i(t)| \, dt \qquad (53)$$

Table 2 shows the values of $\langle |W_i| \rangle$ in milliwatt for the three following configurations

- Output of the gear directly connected to the joint (no spring)
- Optimal linear spring in series with the actuator
- Optimal nonlinear spring in series with the actuator

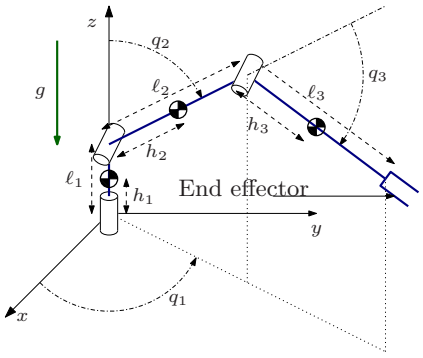


**Fig.**3 3-DOF serial manipulator.

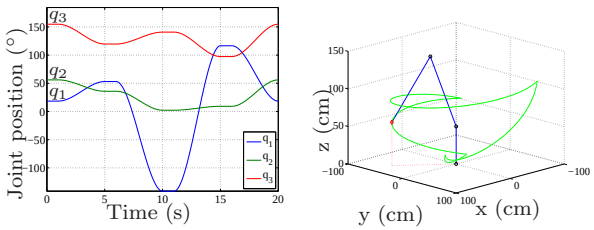


(a) Trajectory (joint space) (b) Path of end effector

**Fig.**4 Joint trajectory and path of the end effector.

**Table** 1 User-defined parameters.

| Parameter | Symbol | Value |
|---|---|---|
| Time horizon | $T$ | $20s$ |
| Number or nodes to interpolate $\overline{w}'_i(\overline{\xi}_i)$ | $N$ | 6 |
| Spring min. displacement range | $\Xi_{i,\min}$ | $2^\circ$ |
| Spring max. displacement range | $\Xi_{i,\max}$ | $70^\circ$ |
| Min. normalized stiffness | $\overline{w}'_{\min}$ | $\tan(2/180\,\pi)$ |
| Max. normalized stiffness | $\overline{w}'_{\max}$ | $\tan(85/180\,\pi)$ |

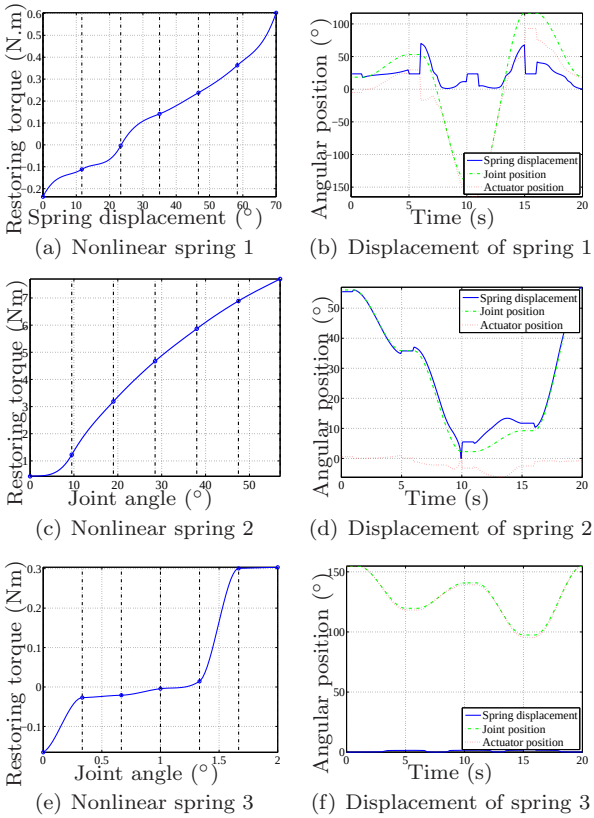


(a) Nonlinear spring 1 (b) Displacement of spring 1
(c) Nonlinear spring 2 (d) Displacement of spring 2
(e) Nonlinear spring 3 (f) Displacement of spring 3

**Fig.**5 Torque profile of the nonlinear springs and angular displacement vs. time.

**Table** 2 Average absolute actuator power (milliwatt).

| $\langle\|W_i\|\rangle$ | Joint 1 | Joint 2 | Joint 3 | Total |
|---|---|---|---|---|
| No spring | 75.6 | 436 | 11.7 | 523 |
| Linear spring | 61.1 | 114 | 11.7 | 187 |
| Nonlinear spring | 52.9 | 29.2 | 11.7 | 93.8 |

From Table 2 we understand that the use of springs in series with the actuators significantly reduces the average mechanical power of the actuators of the joints 1 and 2, and that better results are obtained with nonlinear springs. To better understand the effects of the nonlinear stiffness, we compared in Fig. 6 the speed of the actuator 2 for an optimal linear spring and an optimal nonlinear spring. We can see that the average absolute speed (and thus the mechanical work) is significantly reduced when using a nonlinear spring. In the case of the nonlinear spring, there is a speed peak just before $t = 10s$ but this peak does not significantly contribute to the mechanical work since, as shown in Fig. 7, it occurs when the torque of the spring is very low. For the joint 3, however, the value of $\langle|W_i|\rangle$ is nearly the same for the three configurations *no spring/linear spring/nonlinear spring*. On Fig. 5(e), we see that the optimization algorithm set the displacement range of the spring to the minimum value $\Xi_{i,\min}$ (2°). A possible explanation is that for the joint 3 the introduction of a spring in series with the actuator tends to increase the average actuator power, so the algorithm reduced the displacement range of the spring to the minimum to make the actuator as stiff as possible. A spring with negative stiffness might reduce the actuator power, but this option is forbidden by the constraint (40).

## 6. Technical realization of the nonlinear springs

To realize the nonlinear springs synthesized in Section 5., we use the mechanism shown in Fig. 8. This mechanism consists in a linear spring connected to a cable wound around a non-circular spool which shape is calculated so that the mechanism behaves as a nonlinear rotational spring with the prescribed torque profile [16]. According to Table 2, the use of a spring in series with actuator 3 does not lead to a reduction in the actuator work. Thus, we realize only the nonlinear springs that are in series with actuators 1 and 2, and consider that actuator 3 is rigidly connected to its mechanical joint.

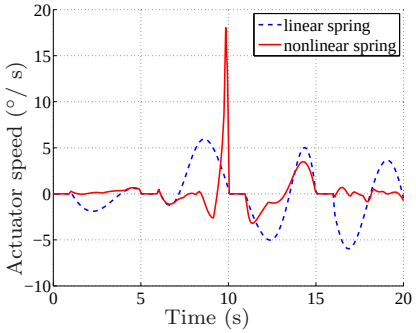


**Fig.**6 Comparison of the speed of the actuator 2 for an optimal linear spring and an optimal nonlinear spring.

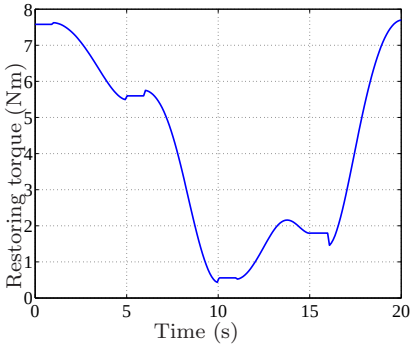


**Fig.**7 Restoring torque of spring 2.

Since this mechanism can only handle positive torques, the nonlinear springs are realized by the antagonistic action of two cable-spool mechanisms. The first ones realizes the torque profiles of Fig. 9(a) and Fig. 10(a), calculated by shifting the torque profiles of Section 5. vertically so that the torque is strictly positive. A reduction ratio is introduced between the joint and the spool to adjust the rotation range of the spool. The second mechanism realizes a constant spring, so that the antagonistic action of the two mechanisms achieves the torque profiles of Section 5.. The shape of the spool synthesizing the shifted torque profiles are shown in Fig. 9(b) and Fig. 10(b). See [16] for the design and realization of the constant springs.

## 7. Conclusions

In this paper, we proposed a general methodology to optimize the nonlinear springs of nonlinear SEAs in order to minimize the mechanical power of the actuators. We showed that, depending on the joint trajectory, the use of springs in series with the actuators significantly reduces the average power of the actuators, and that even better results are obtained when the springs are nonlinear. However for some joint trajec-

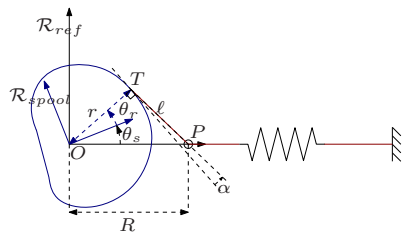


**Fig.**8 Transmission mechanism with a non-circular cable spool.

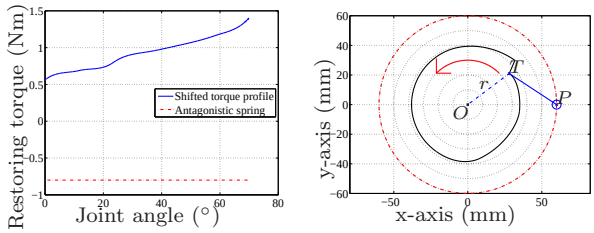


(a) Shifted torque profile (b) Spool

**Fig.**9 Realization of spring 1 with a non-circular spool mechanism.

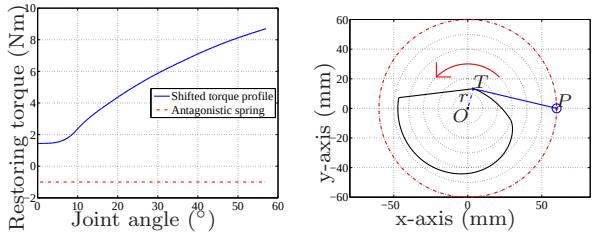


(a) Shifted torque profile (b) Spool

**Fig.**10 Realization of spring 2 with a non-circular spool mechanism.

tory, no optimal spring can be found that reduces the actuator power *and* satisfies the condition of strictly positive stiffness, as it was the case for the 3rd joint. Finally, we showed that the nonlinear springs in series with actuators 1 and 2 of Section 5. can be realized using an antagonistic setup of non-circular cable spool mechanisms.

Future work will focus on improving the design methodology to optimize both the nonlinear springs *and* and the joint trajectory.

## References

[1] Gill A. Pratt and Matthew M. Williamson. "Series elastic actuators". In: *Proc. IEEE International Conference on Intelligent Robots and Systems*. Vol. 1. Washington, DC, USA, 1995, pp. 399–406.

[2] Eduardo Torres-Jara and Jessica Banks. *A Simple and Scalable Force Actuator*. CiteSeerX. 2005.

[3] Bill Bigge and Inman R. Harvey. "Programmable springs: Developing actuators with programmable compliance for autonomous robots". In: *Robotics and Autonomous Systems* 55.9 (2007), pp. 728–734.

[4] S.K. Au, P. Dilworth, and H. Herr. "An ankle-foot emulation system for the study of human walking biomechanics". In: *Proc. IEEE International Conference on Robotics and Automation*. Orlando, Florida, USA, May 2006, pp. 2939–2945.

[5] Antonio Bicchi and Giovanni Tonietti. *Design, Realization and Control of Soft Robot Arms for Intrinsically Safe Interaction with Humans*. Tech. rep. Centro Interdipartimentale di Ricerca "E. Piaggio", Universita di Pisa, Italia, 2002.

[6] Martin Grimmer and Andre Seyfarth. "Stiffness Adjustment of a Series Elastic Actuator in a Knee Prosthesis for Walking and Running: The Trade-off between Energy and Peak Power Optimization". In: *Proc. IEEE/RSJ International Conference on Intelligent Robots and Systems*. Vol. 11. San Francisco, CA, USA, Sept. 2011, pp. 1811–1816.

[7] R. McN. Alexander. "Three uses for springs in legged locomotion". In: *International Journal of Robotics Research* 9.2 (Apr. 1990), pp. 53–61.

[8] Sami Haddadin, Kai Krieger, Mirko Kunze, and Alin Albu-Schäffer. "Exploiting potential energy storage for cyclic manipulation: An analysis for elastic dribbling with an anthropomorphic robot". In: *Proc. IEEE/RSJ International Conference on Intelligent Robots and Systems*. Vol. 11. San Francisco, CA, USA, Sept. 2011, pp. 1789–1796.

[9] E. Suhir. "Shock protection with a nonlinear spring". In: *IEEE Transactions on Components, Packaging, and Manufacturing Technology* 18.2 (June 1995), pp. 430–437.

[10] Jung-Jun Park, Hwi-Su Kim, and Jae-Bok Song. "Safe robot arm with safe joint mechanism using nonlinear spring system for collision safety". In: *Proc. IEEE International Conference on Robotics and Automation*. Kobe, Japan, May 2009, pp. 3371–3376.

[11] K.F. Laurin-Kovitz, J.E. Colgate, and S.D.R. Carnes. "Design of components for programmable passive impedance". In: *Proc. IEEE International Conference on Robotics and Automation*. Vol. 2. Sacramento, California, USA, Apr. 1991, pp. 1476–1481.

[12] S.A. Migliore, E.A. Brown, and S.P. DeWeerth. "Biologically Inspired Joint Stiffness Control". In: *Proc. IEEE International Conference on Robotics and Automation*. Barcelona, Spain, Apr. 2005, pp. 4508–4513.

[13] Ivar Thorson and Darwin Caldwell. "A Nonlinear Series Elastic Actuator for Highly Dynamic Motions". In: *Proc. IEEE/RSJ International Conference on Intelligent Robots and Systems*. Vol. 11. San Francisco, CA, USA, Sept. 2011, pp. 390–394.

[14] V. E. Berbyuk and A. E. Bostrom. "Optimization Problems of Controlled Multibody Systems Having Spring-Damper Actuators". In: *International Applied Mechanics* 37 (7 2001), pp. 935–940.

[15] Nicolas Schmit and Masafumi Okada. "Simultaneous Optimization of Robot Trajectory and Nonlinear Springs to Minimize Actuator Torque". In: *Proc. IEEE International Conference on Robotics and Automation*. St. Paul, MN, USA, May 2012.

[16] Nicolas Schmit and Masafumi Okada. "Design and Realization of a Non-Circular Cable Spool to Synthesize a Nonlinear Rotational Spring". In: *Advanced Robotics* 26 (2012), pp. 235–252.

[17] Alex Barclay, Philip E. Gill, and J. Ben Rosen. "SQP methods and their application to numerical optimal control". In: *Variational calculus, optimal control, and applications*. Ed. by Werner H. Schmidt Leonhard Bittner Rolf Klötzler. Vol. 124. International Series of Numerical Mathematics. Birkhäuser, 1998, pp. 207–222.